

## ENVIRONMENTAL STUDIES

# Temperature sensitivity of SOM decomposition governed by aggregate protection and microbial communities

Shuqi Qin<sup>1,2</sup>, Leiye Chen<sup>1</sup>, Kai Fang<sup>1,2</sup>, Qiwen Zhang<sup>1,2</sup>, Jun Wang<sup>1,2</sup>, Futing Liu<sup>1,2</sup>, Jianchun Yu<sup>1,2</sup>, Yuanhe Yang<sup>1,2\*</sup>

Temperature sensitivity ( $Q_{10}$ ) of soil organic matter (SOM) decomposition is a crucial parameter for predicting the fate of soil carbon (C) under global warming. However, our understanding of its regulatory mechanisms remains inadequate, which constrains its accurate parameterization in Earth system models and induces large uncertainties in predicting terrestrial C-climate feedback. Here, we conducted a long-term laboratory incubation combined with a two-pool model and manipulative experiments to examine potential mechanisms underlying the depth-associated  $Q_{10}$  variations in active and slow soil C pools. We found that lower microbial abundance and stronger aggregate protection were coexisting mechanisms underlying the lower  $Q_{10}$  in the subsoil. Of them, microbial communities were the main determinant of  $Q_{10}$  in the active pool, whereas aggregate protection exerted more important control in the slow pool. These results highlight the crucial role of soil C stabilization mechanisms in regulating temperature response of SOM decomposition, potentially attenuating the terrestrial C-climate feedback.

## INTRODUCTION

Globally, approximately 2300 Pg (1 Pg =  $10^{15}$  g) carbon (C) is stored in the top 3 m of soils, of which more than 70% is distributed in deep horizons below 20 cm (1). Deep soil C is characterized by high stability over long time scales, because the rate of soil organic matter (SOM) decomposition usually decreases with soil depth (2). Similar to many other biochemical reactions, the decomposition of SOM is temperature dependent (3). Because of this point, global warming is expected to promote carbon dioxide ( $\text{CO}_2$ ) release from both the topsoil and the subsoil, thereby triggering a potential positive feedback (4, 5). However, large uncertainties remain in the magnitude of this C-climate feedback, partly due to the inaccurate parameterization of the temperature sensitivity ( $Q_{10}$ ) of SOM decomposition in different soil depths and C pools in Earth system models (ESMs) (3, 6). It has been estimated that the current use of a globally constant  $Q_{10}$  value in most models underestimates the magnitude of C-climate feedback by 25% compared to incorporating the spatially heterogeneous  $Q_{10}$  values into models (7). Therefore, a deeper understanding of the fundamental mechanisms regulating  $Q_{10}$  is pivotal for accurately predicting soil C dynamics and reducing model uncertainties in forecasting terrestrial C-climate feedback.

Historically, SOM quality had been recognized as the major determinant of  $Q_{10}$ . On the basis of enzyme kinetic theory, “carbon-quality temperature” hypothesis predicts that the decomposition of low-quality substrates in the subsoil requires high activation energy and is thus more sensitive to temperature changes (8, 9). However, several emergent conceptual frameworks have challenged the perceived importance of soil C quality in governing the decomposition of SOM and its responses to warming, and argued that processes controlling substrate accessibility (e.g., SOM protection, spatial disconnection, and enzyme diffusion) are also critically important (10–13). Moreover, microbial properties (e.g., microbial abundance, community composition, and enzyme productions) and the existence of energetic barriers to microorganisms regulate

SOM decomposition and  $Q_{10}$  as well (2, 10, 14, 15). Despite the theoretical predictions of an important role for these factors, direct evidence for the effects of SOM protection and microbial communities on  $Q_{10}$  is scarce (16), which, in turn, limits the accurate parameterization of  $Q_{10}$  in ESMs. The soil profile provides an ideal natural gradient for exploring the relative contribution of different mechanisms underlying  $Q_{10}$  due to vertical variations in substrate quality and environmental and microbial controls over SOM decomposition (9, 17, 18). Moreover, manipulative experiments such as aggregate disruption experiments (19) and microorganism reciprocal transplant experiments (20), combined with laboratory culture, offer the possibility to explore the effects of aggregate protection and microbial communities on  $Q_{10}$ , respectively. However, these approaches have not been adequately applied in disentangling the complex mechanisms regulating  $Q_{10}$  between soil depths.

It is widely recognized that the large heterogeneity of SOM decomposition and its response to warming exists not only between soil depths but also within the composition of SOM itself (16, 21, 22). SOM is considered as a heterogeneous mixture consisting of pools with different turnover times, which is also the premise of classic soil C models such as Century (23) and RothC (24). It has been assumed that the active C pool, persisting for hours to weeks, is composed mainly of chemically labile and unprotected compounds, whereas the slow C pool could persist for decades to centuries due to the physicochemical and biological constraints on decomposition (13). These variations in substrate quality and abiotic and biotic regulators between C pools imply that their responses to climate warming and the associated mechanisms may also differ (12). Despite this recognition, current models assume equal  $Q_{10}$  value for all C pools (3). The assumption of a single  $Q_{10}$  value may obscure the responses of soil C pool to climate warming, especially for the slow C pool, whose temperature response cannot be well captured from short-term incubation experiments (21, 25). With the development of a data-model fusion technology, Bayesian probabilistic inversion, it is possible to estimate  $Q_{10}$  values for different soil C pools through the combination of long-term incubations and two-pool models (26). Nonetheless, limited studies have adopted this approach to explore potential mechanisms regulating  $Q_{10}$  for different soil C pools.

<sup>1</sup>State Key Laboratory of Vegetation and Environmental Change, Institute of Botany, Chinese Academy of Sciences, Beijing 100093, China. <sup>2</sup>University of Chinese Academy of Sciences, Beijing 100049, China.

\*Corresponding author. Email: yhyang@ibcas.ac.cn

This study aimed to address the following three questions: (i) Are  $Q_{10}$  values for bulk soil, active C pool, and slow C pool different between the topsoil and the subsoil? (ii) What are the regulatory mechanisms underlying the  $Q_{10}$  difference between soil depths? (iii) Are the regulatory mechanisms different between the two C pools? To answer these questions, topsoil samples from 0 to 10 cm depth and subsoil samples from 30 to 50 cm depth were collected from three alpine meadow sites on the Tibetan Plateau (fig. S1). On the basis of these samples, we conducted a 330-day incubation experiment, in combination with three methods (bulk soil  $Q_{10}$  by average decomposition rate,  $Q_{10}$  values for different respired soil C fractions through the  $Q_{10-q}$  method, and active and slow pool  $Q_{10}$  by the two-pool model), to estimate the  $Q_{10}$  values of various SOM components for the two soil depths. Soil properties including substrate quality, SOM protection, and microbial characteristics were then quantified to explore the determinants of  $Q_{10}$ . We further performed two manipulative experiments (i.e., aggregate disruption experiment and microorganism reciprocal transplant experiment) to examine the effects of aggregate protection and microbial communities on  $Q_{10}$  in different C pools.

## RESULTS

### Differences in $Q_{10}$ values between soil depths

Bulk soil  $Q_{10}$  in the topsoil was estimated at 2.1 on average, significantly higher than the value (1.8) in the subsoil ( $P < 0.05$ ; Fig. 1A). No significant interactions between site and depth were observed, demonstrating that the depth effect on  $Q_{10}$  was independent of the sampling site ( $P = 0.28$ ; table S1). To further explore  $Q_{10}$  for various SOM components, we adopted the  $Q_{10-q}$  method to evaluate  $Q_{10}$  for three soil C fractions (i.e., 1 to 1.5%, 2 to 2.5%, and 3 to 3.5% of cumulative respired soil C), which represent a gradient of decreasing substrate lability. Similarly, the topsoil  $Q_{10}$  was significantly higher than the subsoil for 2 to 2.5% and 3 to 3.5% of cumulative respired soil C ( $P < 0.05$ ; Fig. 1B), without interaction effects ( $P = 0.20$  and 0.50, respectively; table S1). No significant difference was detected in the  $Q_{10}$  value of 1 to 1.5% of cumulative respired soil C between soil depths ( $P = 0.05$ ; table S1). In addition,  $Q_{10}$  estimated from the two-pool model also showed significantly lower values in the subsoil for both active pool and slow pool ( $P < 0.05$ ; Fig. 1A), with no site  $\times$  depth interaction ( $P = 0.31$  and 0.26 for active pool and slow pool, respectively; table S1).

### Determinants of the $Q_{10}$ difference between soil depths

To explore determinants of the  $Q_{10}$  difference between soil depths, we analyzed four types of variables associated with  $Q_{10}$ , including substrate quality, SOM association with minerals, SOM protection by aggregates, and microbial communities, and compared them between the two soil depths. Of these variables, substrate quality revealed by SOM composition differed between the topsoil and the subsoil. Specifically, the intensity of O-alkyl C acquired from solid-state  $^{13}\text{C}$  CPMAS (cross polarization with magic-angle spinning) NMR (nuclear magnetic resonance) was higher in the topsoil (41%) than in the subsoil (29%) ( $P < 0.01$ ; Fig. 2, A and B), whereas the contribution of alkyl C was significantly higher in the subsoil (53%) than in the topsoil (28%) ( $P < 0.01$ ; Fig. 2, A and B). The calculated alkyl/O-alkyl ratio was thus significantly higher in the subsoil ( $P < 0.01$ ; Fig. 2B), indicating more recalcitrant SOM in deep soils. Consequently, on the basis of the “carbon-quality temperature” hypothesis, the poorer substrate quality could not be responsible for the lower  $Q_{10}$  in the subsoil.

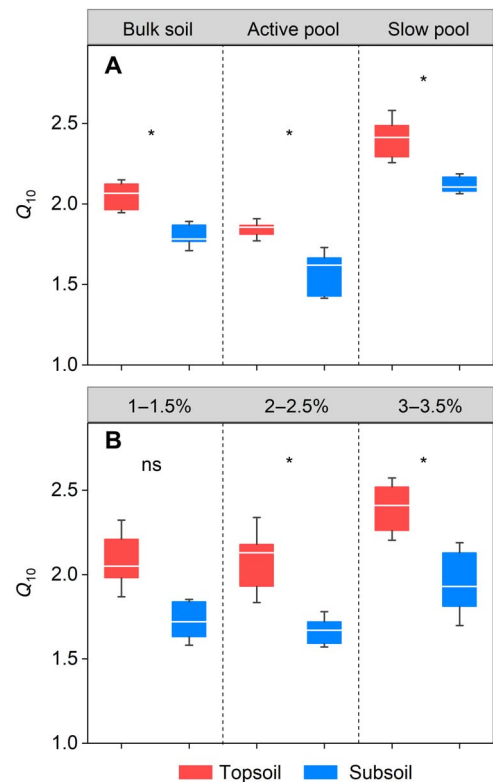


**Fig. 1.  $Q_{10}$  values for various SOM components in the topsoil and subsoil. (A)**  $Q_{10}$  for bulk soil, active pool, and slow pool. **(B)**  $Q_{10}$  for three cumulative respired soil C fractions. The ends of the boxes represent the 25th and 75th percentiles. The horizontal lines inside each box and the whiskers show the median and the SD, respectively ( $n = 9$ ). \* $P < 0.05$ , significant difference between the topsoil and the subsoil; ns, no significant difference.

We then measured the proportion of soil organic carbon (SOC) associated with Fe to total SOC (i.e., Fe-bound SOC) to quantify SOM protection by minerals. The results revealed no significant difference in the Fe-bound SOC between the topsoil and the subsoil ( $P = 0.17$ ; Fig. 2C). In consistence, the proportion of SOC associated with silt + clay ( $< 53 \mu\text{m}$ ) acquired by the wet-sieving technique did not show significant difference ( $P = 0.83$ ; Fig. 2C), jointly indicating that SOM protection by minerals might be less responsible for the  $Q_{10}$  difference between soil depths. However, SOM protection by aggregates, as determined by the same technique, differed between the two soil depths. Compared with the topsoil, the proportion of SOC distribution in the subsoil was lower in macroaggregates (250 to 2000  $\mu\text{m}$ , 44% versus 63%,  $P < 0.01$ ; Fig. 3A) but higher in microaggregates (53 to 250  $\mu\text{m}$ , 32% versus 15%,  $P < 0.01$ ; Fig. 3B). Moreover, as revealed by linear regression analyses, these differences in aggregate protection were associated with the  $Q_{10}$  differences between soil depths. Bulk soil  $Q_{10}$ , active pool  $Q_{10}$ , and slow pool  $Q_{10}$  all increased with the proportion of SOC distributed in macroaggregates (Fig. 3, A, C, and E) but decreased with the proportion in microaggregates (Fig. 3, B, D, and F).

Microbial communities, as determined through phospholipid fatty acid (PLFA) analysis, also differed between the topsoil and the subsoil. The abundances of the microbial groups, including total PLFAs, bacterial PLFAs, and fungal PLFAs, were all higher in the topsoil than in the subsoil ( $P < 0.01$ ; table S2). The community structure was different in

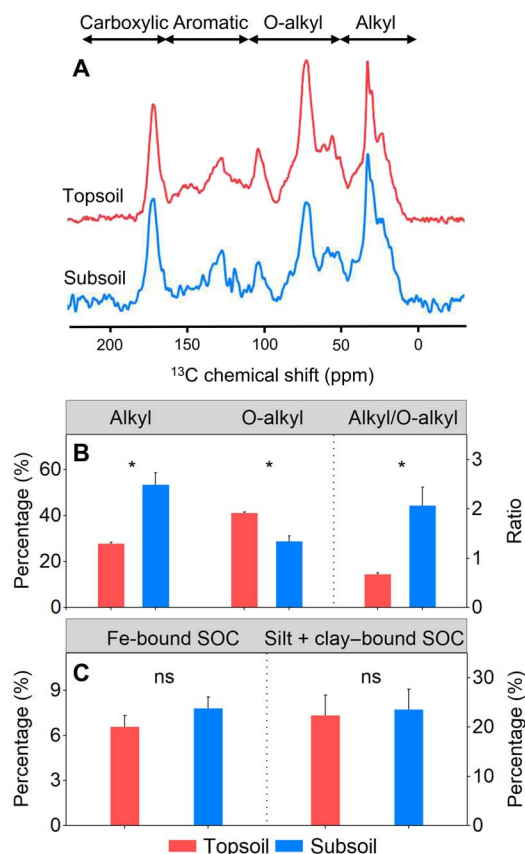


**Fig. 2. Comparison of SOM composition and mineral protection between the topsoil and the subsoil.** (A)  $^{13}\text{C}$  CPMAS NMR spectra. Chemical shifts of 0 to 50, 50 to 110, 110 to 165, and 165 to 220 parts per million (ppm) represent alkyl C, O-alkyl C, aromatic C, and carboxylic C, respectively. (B) Percentage of alkyl C and O-alkyl C relative to total SOC and ratio of the two SOM compositions. (C) Percentage of Fe-bound SOC and silt + clay-bound SOC relative to total SOC. Error bars denote SE ( $n = 9$ ). \* $P < 0.01$ , significant difference between the topsoil and the subsoil. ns, no significant difference.

certain aspects, with significantly higher fungal/bacterial (F/B) ratio ( $P < 0.05$ ) and relative abundance of fungal PLFAs (fungal PLFAs/total PLFAs,  $P < 0.01$ ) in the topsoil (table S2), while there was no difference in the relative abundance of bacterial PLFAs (bacterial PLFAs/total PLFAs) between the two depths ( $P = 0.10$ ; table S2). These variations in microbial communities also contributed to the  $Q_{10}$  differences: Bulk soil  $Q_{10}$ , active pool  $Q_{10}$ , and slow pool  $Q_{10}$  were all positively associated with the relative abundance of fungal PLFAs (Fig. 4, A to C).

### Mechanisms of depth-associated variations in $Q_{10}$ in various C pools

To test whether the underlying mechanisms of depth-associated variations in  $Q_{10}$  were C pool dependent, we conducted variation partitioning analyses for the active and slow C pools. During these analyses, we incorporated aggregate protection and microbial communities, which exerted significant controls over  $Q_{10}$  (Figs. 3 and 4). The results demonstrated that  $Q_{10}$  variations in the bulk soil and slow pool were primarily explained by aggregate protection, with the pure effects being 24.5% (Fig. 5A) and 36.9% (Fig. 5C), respectively. The  $Q_{10}$  variations in the active pool, however, were mainly explained by microbial communities, whose pure effect was 16.2% (Fig. 5B). These

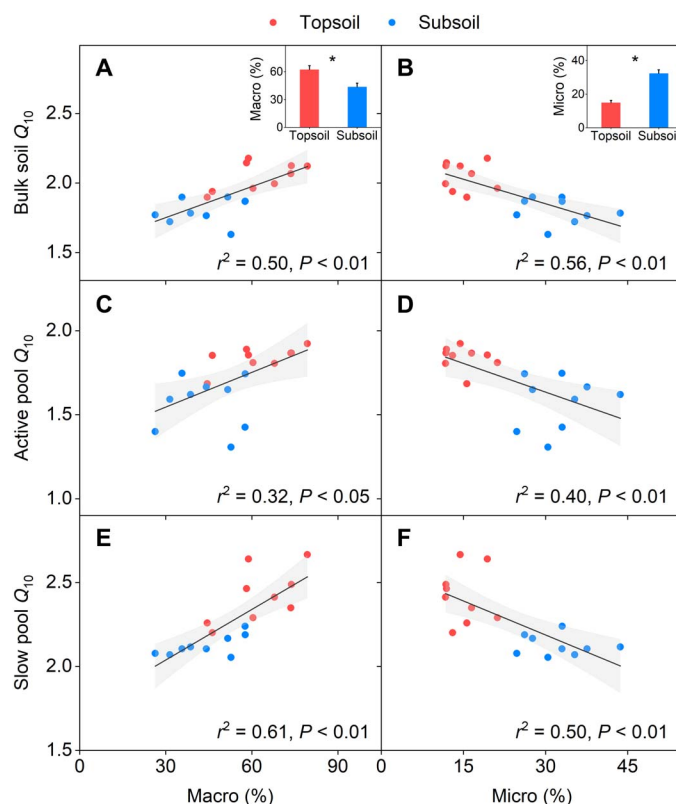


**Fig. 3. Relationships between  $Q_{10}$  and C distribution in aggregates.** (A and B) Bulk soil  $Q_{10}$  with macro and micro. (C and D) Active pool  $Q_{10}$  with macro and micro. (E and F) Slow pool  $Q_{10}$  with macro and micro. Macro refers to the percentage of soil C stored in macroaggregates (250 to 2000  $\mu\text{m}$ ), and micro denotes the percentage in microaggregates (53 to 250  $\mu\text{m}$ ). Red circles represent samples in the topsoil ( $n = 9$ ), and blue circles represent samples in the subsoil ( $n = 9$ ).  $r^2$  is the proportion of variance explained. The insets show the depth-associated variations of C distribution in macroaggregates and microaggregates, respectively. Error bars denote SE ( $n = 9$ ). \* $P < 0.01$ , significant difference between the two soil depths.

results demonstrated that microbial communities governed  $Q_{10}$  in the active pool, while aggregate protection governed  $Q_{10}$  in the slow pool.

The different underlying mechanisms of  $Q_{10}$  between the two C pools were confirmed by the microorganism reciprocal transplant experiment and aggregate disruption experiment. The former experiment showed that, in the active pool, inoculating the topsoil with the subsoil microorganism (away inoculum) significantly decreased  $Q_{10}$  compared with its own inoculum ( $P < 0.01$ ; fig. S2A), whereas inoculating the subsoil with the topsoil microorganism (away inoculum) resulted in a significantly higher  $Q_{10}$  ( $P < 0.01$ ; fig. S2A). Consequently,  $\Delta Q_{10}$  (i.e.,  $Q_{10 \text{ topsoil}} - Q_{10 \text{ subsoil}}$ ) was significantly lower for the treatment of away inoculum in the active pool ( $P < 0.01$ ; Fig. 6A). However, in the slow pool, no significant difference was detected between the two inoculums in both the topsoil and the subsoil ( $P = 0.88$  and  $0.21$ , respectively; fig. S2B), and thus, no change was observed for  $\Delta Q_{10}$  in this pool ( $P = 0.20$ ; Fig. 6A). In contrast, the later experiment demonstrated that the SOM protection by aggregates mainly affected  $Q_{10}$  in the slow pool. The removal of aggregate protection by crushing resulted in a significantly declined  $\Delta Q_{10}$  in the slow pool ( $P < 0.01$ ) but had no effect in the active pool ( $P = 0.21$ ; Fig. 6B).

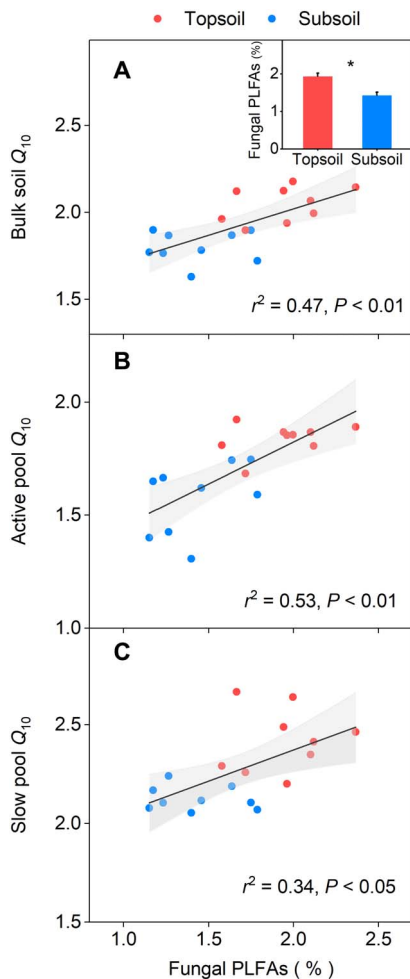


**Fig. 4. Relationships between  $Q_{10}$  and fungal PLFAs.** (A) Bulk soil  $Q_{10}$ . (B) Active pool  $Q_{10}$ . (C) Slow pool  $Q_{10}$ . Fungal PLFAs refer to the relative abundance of fungi (fungal PLFAs/total PLFAs). Red circles represent samples in the topsoil ( $n = 9$ ), and blue circles represent samples in the subsoil ( $n = 9$ ).  $r^2$  is the proportion of variance explained. The inset shows the comparison of relative abundance of fungal PLFAs between the topsoil and the subsoil.  $*P < 0.01$ . Error bars are SE ( $n = 9$ ).

## DISCUSSION

Our results demonstrate that SOM decomposition in the topsoil was more sensitive to warming than in the subsoil. This significant difference could be due to the following two reasons. First, the stronger SOM protection by aggregates in the subsoil could attenuate  $Q_{10}$ . Aggregate protection exerts important control over the stabilization of SOM (27), and it has been reported that small sizes of aggregates need more energy to be disrupted (11). That is to say, the degree of protection increases with the decline in aggregate sizes and would be stronger in microaggregates (27). In our study, a higher proportion of C stored in microaggregates in the subsoil compared with the topsoil indicated that aggregate protection was stronger in the subsoil, which further resulted in a lower  $Q_{10}$  value through the following two aspects. On the one hand, SOM is occluded in the interior of microaggregates, inducing spatial disconnection between substrates and enzymes, and thus protecting SOM from microbial decomposition (27). On the other hand, the small sizes of microaggregates could restrict the diffusion of oxygen (11), which limits the activity of microorganisms and results in low  $Q_{10}$  (28). Overall,

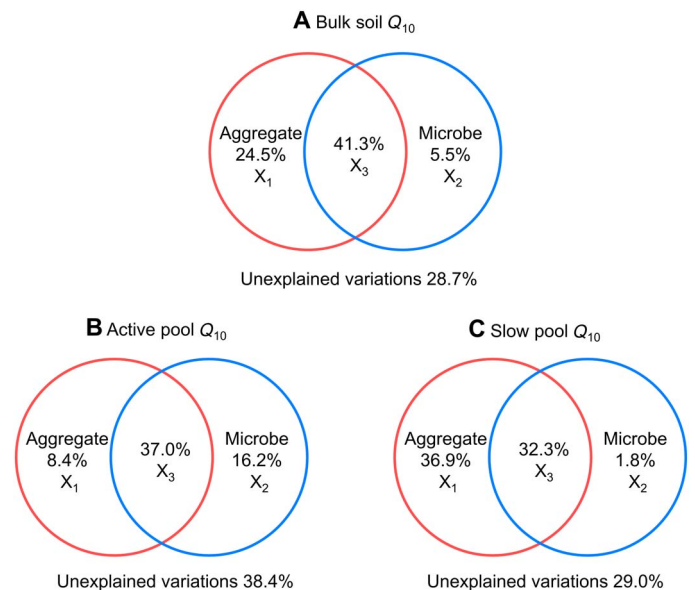


**Fig. 5. Variation partitioning analyses for  $Q_{10}$  in various SOM components.** (A) Bulk soil  $Q_{10}$ . (B) Active pool  $Q_{10}$ . (C) Slow pool  $Q_{10}$ . The variation is partitioned to the following fractions: pure effect of aggregate protection ( $X_1$ ), pure effect of microbial communities ( $X_2$ ), joint effects of aggregate protection and microbial communities ( $X_3$ ), and unexplained variations. Aggregate protection includes the percentage of soil C stored in macroaggregates (250 to 2000  $\mu\text{m}$ ) and microaggregates (53 to 250  $\mu\text{m}$ ). Microbial communities refer to the relative abundance of fungal PLFAs.

the determining role of SOM protection by aggregates observed here, together with previous proposals (3, 10), jointly demonstrates the importance of aggregate protection in governing the response of SOM decomposition to global warming.

Second, variations in microbial communities between soil depths could lead to the  $Q_{10}$  difference. Microorganisms are addressed to play key roles in regulating the terrestrial C cycle, mediating not only the rate of SOM decomposition but also its responses to warming (14). In our study, the lower microbial abundance in the subsoil (table S2) that resulted from the alterations in soil resource availability (e.g., the decline in soil C and nitrogen; table S3) might constrain SOM decomposition even under high temperature and thus attenuate  $Q_{10}$  (15). Moreover, microbial community composition would also affect  $Q_{10}$ . It has been reported that fungi are the dominant decomposers of recalcitrant substrates (29). Because the decomposition of these low-quality substrates requires greater activation energy (8), the shift in microbial community composition with decreasing proportion of fungi with soil depth may contribute to the lower  $Q_{10}$  in the subsoil (30). These deductions were further confirmed by the microorganism reciprocal transplant experiment: By applying inoculums with high microbial abundance and fungi proportion to the subsoil,  $Q_{10}$  significantly increased, while applying inoculums with low microbial abundance and fungi proportion to the topsoil significantly decreased  $Q_{10}$  (fig. S2A). In addition to the variations in microbial communities, the activities of subsoil microorganisms might not be sustained by enough energy due to the lack of fresh substrates (2, 31, 32), which would further attenuate  $Q_{10}$  in the subsoil (33).

Our results also demonstrated that the  $Q_{10}$  variation in the active pool was primarily mediated by microbial communities, whereas the

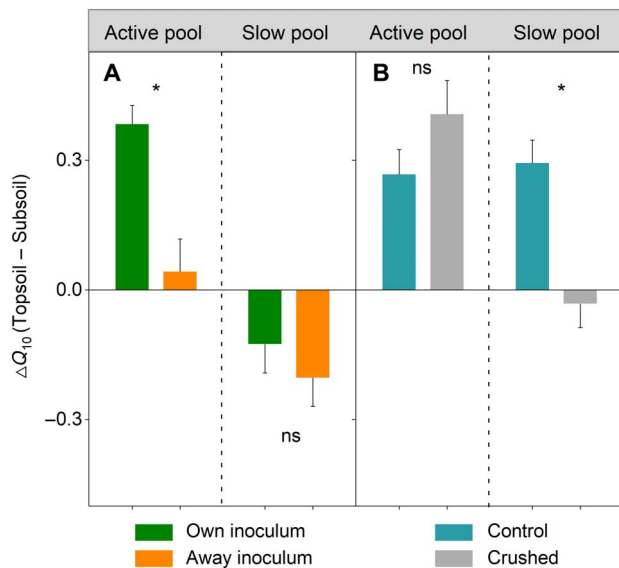


**Fig. 6.  $\Delta Q_{10}$  in active and slow pools derived from two manipulative experiments. (A) Microorganism reciprocal transplant. (B) Aggregate disruption.**  $\Delta Q_{10}$  is the  $Q_{10}$  difference between the topsoil and the subsoil, with a positive value representing larger  $Q_{10}$  in the topsoil and a negative value representing larger  $Q_{10}$  in the subsoil. Error bars denote SE ( $n = 9$ ). \* $P < 0.01$ , significant difference between control and treatment. ns, no significant difference.

$Q_{10}$  variation in the slow pool was mainly explained by aggregate protection. The difference in the underlying mechanisms between C pools could be largely due to their distinct physicochemical and biological properties. To be specific, most compounds in the active pool are unprotected and thus more accessible to microorganisms (13). The high substrate availability indicates that the decomposition of these unprotected SOM and their responses to warming are mainly related to microbial communities (27), especially for the subsoil, where low microbial abundance and fungal proportions could limit the decomposition activity under a warming scenario (15). By contrast, in the slow pool, most compounds are preserved with the protection of soil minerals and aggregates (11). Even in the presence of high-quality substrates and a competent microbial community, aggregates could prevent the contact of substrates and microorganisms and constrain the responses of SOM decomposition to warming (3, 10). Consequently, the level of SOM protection by aggregates becomes the major determinant of  $Q_{10}$  in the slow pool. Nevertheless, other properties might also be distinct among soil C pools and thus function differently in regulating  $Q_{10}$  of various SOM components, such as the dynamics of enzyme pools (34) and the energetic signatures of substrates (35), which need to be addressed in future studies.

Although our study provided empirical evidence for the mechanisms underlying  $Q_{10}$ , there are still some limitations. First, in addition to the mechanisms considered in this study, other biotic and abiotic controls such as the energetic constraints of microorganisms (2, 31, 32, 35), the dynamics of enzyme pools and their catalytic power (34), the spatial separation of substrates (36), and the diffusion of enzymes and oxygen (11) could also regulate SOM decomposition and its temperature response. Extending studies incorporating these factors are deserved to gain further understanding on this issue. Second, despite a widely used sterilization technique with limited effects on soil physical properties,  $\gamma$ -irradiation would affect soil chemical

properties through the release of labile C (37). Moreover, noncellular processes, which have been considered important in  $\text{CO}_2$  production (38, 39), were not determined in the current sterilization experiment. Future studies should thus aim to better differentiate the effects of substrates and microorganisms and also evaluate the contribution of non-cellular processes to soil C release and their temperature responses. Third, the  $Q_{10}$  values of different soil C pools were estimated from a first-order kinetic model without representing other controls on SOC dynamics, such as microbial growth, activities, turnover, and C use efficiency (40, 41); enzyme activities and dynamics (34, 42); organic matter–mineral interactions (6); and hydrologically driven diffusion of substrates or enzymes (43). In view of the simple assumption about soil C turnover in current models, uncertainties might exist in model estimations. Hence, future studies should improve model structure to better reflect the mechanisms of soil C stabilization (6) and also measure  $Q_{10}$  of different soil C pools directly to provide benchmark for model development.

In summary, through a multiple approach–based analysis, we observed that, across soil depths, lower microbial abundance and stronger SOM protection by aggregates are two coexisting mechanisms responsible for the lower  $Q_{10}$  in the subsoil. We also found that the underlying mechanisms of  $Q_{10}$  were different between the active and slow pools, as microbial communities dominated in the active pool, whereas aggregate protection was more important in the slow pool. Given that the slow C pool is the largest component of SOM with a longer turnover time, SOM protection via microaggregates could be the key mechanism that regulates the long-term response of SOM decomposition to global warming. Overall, these findings imply that the existence of soil C stabilization mechanisms could reduce the effect of climate warming on SOM decomposition, especially for the large deep and slow C pools, thereby attenuating the predicted terrestrial C–climate feedback.

## MATERIALS AND METHODS

### Site description and soil sampling

We collected soil samples from three alpine meadow sites on the Tibetan Plateau, China, where substantial quantities of soil organic C (15.3 Pg) were stored in the top 3 m (44). In the past decades, mean annual temperature on the plateau increased at a rate about twice that of global warming (45). The high rate of climate warming, together with the high  $Q_{10}$  on the plateau (46), could induce potential positive C–climate feedback in this unique geographic region. Moreover, because of the detected differences in substrate quality, environmental constraints, and microbial properties among soil depths (17), there might be considerable differences in  $Q_{10}$  through soil profile. To test this possibility, we selected three sampling sites (Halejing, Xihetai, and Zhagamu) on the northeastern Tibetan Plateau (fig. S1A) and examined  $Q_{10}$  in different soil depths and various soil C components, as well as the associated mechanisms.

The sites are situated at latitudes of 37.02°N to 37.61°N and longitudes of 100.11°E to 101.24°E, with an elevation of 3200 to 3400 m. The mean annual temperature varies from 0.12° to 2.20°C, and the mean annual precipitation ranges from 340 to 378 mm. The vegetation type belongs to alpine meadow, characterized by the dominant species of *Kobresia pygmaea* in Halejing and Zhagamu, and *Kobresia humilis* in Xihetai. The soil type at the three study sites is Cambisol according to the World Reference Base for Soil Resources (46). Cambisols are widespread not only on the Tibetan Plateau but also worldwide (47), accounting for ~38% of the Tibetan Plateau and ~11% of the

global land surface. Soil physicochemical properties at these sites are given in table S3.

We conducted soil sampling in July and August 2014 (44). At each sampling site, we set up a 10 m × 10 m square plot and excavated three replicate soil pits at two corners and the center along a diagonal line (fig. S1B). We then collected topsoil at depths of 0 to 10 cm and subsoil at depths of 30 to 50 cm (fig. S1C). Soils from each depth were divided into two subsamples: one of which was passed through a 2-mm sieve and stored at −20°C to determine SOM composition and microbial communities; the other set was air-dried and processed for measurements of other physicochemical properties.

### Experimental design

To examine the  $Q_{10}$  difference between soil depths and the associated mechanisms, we established two manipulative experiments based on 330-day incubations at 10° and 20°C: One was conducted to compare  $Q_{10}$  in the topsoil and subsoil, and also to test the effects of aggregate protection through the uncrushed (control) and crushed (remove aggregate protection) soils (termed “aggregate disruption experiment”). The other was performed to examine the depth difference in microbial controls by inoculating soils with active microorganism from away (collected in the other depth) and own (the same depth) (termed “microorganism reciprocal transplant experiment”).

In the aggregate disruption experiment, we compared  $Q_{10}$  between the topsoil and the subsoil and then examined the effects of aggregate protection on  $Q_{10}$ . The treatments included uncrushed (control) and crushed soil samples. For the crushed treatment, air-dried soil samples were crushed for 1 min by a ball mill to disrupt aggregates and remove aggregate protection (19). Together, a 3 × 2 × 2 × 3 factorial experiment was conducted corresponding to three study sites, two soil depths, two levels of aggregate disruption, two incubation temperatures, and three replicates. For each of these treatments, 10 g of air-dried topsoil and 20 g of air-dried subsoil from each replicate were evenly distributed into 250 ml of airtight amber jars and incubated at both 10° and 20°C for 330 days (fig. S1D). Soil moisture was adjusted to 60% of water holding capacity (46). The rate of CO<sub>2</sub> release was determined on the basis of the changes in headspace CO<sub>2</sub> concentration during the incubation interval (17) using an infrared gas analyzer (EGM-5; PP Systems, Haverhill, MA, USA). The measurements were taken every 1 to 4 days for the first 3 weeks and then 1 to 2 weeks for 3 months, followed by 1 to 2 months for the rest of the incubation. It should be noted that the CO<sub>2</sub> production from the uncrushed (control) soils was also used to explore the difference in  $Q_{10}$  between soil depths.

In the microorganism reciprocal transplant experiment, we explored whether microorganisms were functionally different between soil depths (20). This experiment was conducted by applying two microbial inoculums (derived from topsoil and subsoil) to both sterilized topsoil and subsoil. Specifically, soil samples were sterilized using  $\gamma$ -irradiation (<sup>60</sup>Co) at a dose of 30 kGy (37). The sterilized soil was then divided into two subsamples, receiving the inoculum derived from itself (own) and from the other corresponding depth (away), respectively; the former treatment (own) was treated as control. In total, 72 microcosms (3 sites × 2 soil depths × 2 inoculums × 2 temperatures × 3 replicates) were constructed. Inoculums from each soil depth were made by adding 1 g of dry weight fresh soil to 100 ml of sterilized deionized water. Then, the inoculum was shaken at 150 rpm for 0.5 hour and filtered through a Whatman GF/C filter. Inoculum (0.4 ml) was applied to per gram soil. The procedure of subsequent CO<sub>2</sub> measurement was the same as the first experiment.

### Calculation of $Q_{10}$ values

We adopted three methods to calculate  $Q_{10}$  values for bulk soil and various SOM components. First,  $Q_{10}$  for bulk soil was calculated according to the decomposition rate at two incubation temperatures

$$Q_{10} = (R_w/R_c)^{10/(T_w-T_c)} \quad (1)$$

where  $R_w$  and  $R_c$  denote the average rate of SOM decomposition at the warmer and colder temperature (mg CO<sub>2</sub>-C g<sup>-1</sup> SOC day<sup>-1</sup>), respectively.  $T_w$  and  $T_c$  represent the warmer and colder temperature (°C).  $Q_{10}$  obtained by this method was referred to as bulk soil  $Q_{10}$ .

Second, the  $Q_{10-q}$  method, which is based on the measured cumulative percentage of soil C respired during incubation, was applied to calculate the  $Q_{10}$  values of different SOM fractions (22)

$$Q_{10-q} = (t_c/t_w)^{10/(T_w-T_c)} \quad (2)$$

where  $t_c$  and  $t_w$  are the time needed to decompose a given soil C fraction at the colder and warmer temperature (day), respectively.  $T_w$  and  $T_c$  denote the warmer and colder temperature (°C). In this study, we chose the upper limit of soil C fraction according to the lowest cumulative percentage of respired C at 10°C (3.9%; fig. S3), which was within the range of previous incubations (0.4 to 17.0%) based on the same temperature and the approximate duration (48, 49). According to a previous study (16), we then set the size of the fractions as 0.5% of total soil C and estimated  $Q_{10}$  values for three fractions of soil C (i.e., 1 to 1.5%, 2 to 2.5%, and 3 to 3.5% of cumulative respired soil C), which represent a gradient of decreasing substrate lability.

Last, we used a two-pool (that is, active and slow pools with different turnover times) model to estimate  $Q_{10}$  for each C pool using data from our 330-day incubation experiment. The two-pool model performed well in simulating the soil C flux (fig. S4) and was applied to each sample at the two temperatures as follows (26)

$$R_{(t)} = \sum_{i=1}^2 k_i f_i C_{\text{tot}} e^{-k_i t} \quad (3)$$

$$Q_{10}^i = \left( \frac{k_i(T_w)}{k_i(T_c)} \right)^{\frac{10}{T_w-T_c}} \quad (4)$$

$$f_1 + f_2 = 1 \quad (5)$$

where  $R_{(t)}$  is the measured decomposition rate at time  $t$  (mg CO<sub>2</sub>-C g<sup>-1</sup> SOC day<sup>-1</sup>).  $C_{\text{tot}}$  denotes the initial SOC content (i.e., 1000 mg C g<sup>-1</sup> SOC),  $k_1$  and  $k_2$  are the decay rates of active and slow pool (day<sup>-1</sup>), and  $f_1$  and  $f_2$  denote the fractions of the active pool and slow pool.  $Q_{10}^1$  and  $Q_{10}^2$  represent  $Q_{10}$  in the active pool and slow pool.  $k_i(T_w)$  and  $k_i(T_c)$  are the decay rates at the warmer ( $T_w$ ) and colder ( $T_c$ ) temperature, respectively. Before modeling, the prior range of the five parameters ( $k_1$  and  $k_2$  at 10°C,  $Q_{10}^1$ ,  $Q_{10}^2$ , and  $f_1$ ; table S4) was set on the basis of previous studies (17, 50) and then determined by a Markov chain Monte Carlo (MCMC) approach as follows (26): Probabilistic inversion approach based on Bayes' theorem (Eq. 6) was applied to optimize parameters (8) in the model. In this approach, the posterior probability density

function (PDF)  $P(\theta|Z)$  was acquired from the prior knowledge of parameters and the information of incubation data, represented by a prior PDF  $P(\theta)$  and a likelihood function  $P(Z|\theta)$ , respectively

$$P(\theta|Z) \propto P(Z|\theta)P(\theta) \quad (6)$$

To calculate the likelihood function  $P(Z|\theta)$ , we assumed that errors between modeled and observed values followed a multivariate Gaussian distribution with a zero mean

$$P(Z|\theta) \propto \exp\left\{-\sum_{i=1}^2 \sum_{t \in \text{obs}(Z_i)} \frac{[Z_i(t) - X_i(t)]^2}{2\sigma_i^2(t)}\right\} \quad (7)$$

where  $Z_i(t)$  and  $X_i(t)$  denote the measured and modeled data, and  $\sigma_i(t)$  represents the SD of the measurements. Metropolis-Hastings (M-H) algorithm, an MCMC technique, was used to complete the construction of  $P(\theta|Z)$  of parameters (51, 52).

### Measurements of abiotic and biotic variables associated with $Q_{10}$

We determined four types of variables, including substrate quality, SOM association with minerals, SOM protection by aggregates, and microbial communities, to explore potential mechanisms responsible for the  $Q_{10}$  difference between the two soil depths. Specifically, to determine substrate quality, SOM composition was investigated by solid-state  $^{13}\text{C}$  CPMAS NMR. Having been treated with 10% hydrofluoric acid (HF) repeatedly (53), soil samples were rinsed with deionized water and then freeze-dried. Approximately 100 mg of HF-treated samples was measured on an AVANCE III 400 WB spectrometer (Bruker BioSpin, Rheinstetten, Baden-Württemberg, Germany) at 100.62 MHz. The spectrometer was equipped with a 4-mm CPMAS probe, and the parameters were set with a spinning rate of 8 kHz, a contact time of 2 ms, and a recycle delay of 6 s. We then used MestReNova 9.0 (Mestrelab Research S.L., Santiago de Compostela, Galicia, Spain) to integrate the spectra into the following chemical shift regions and acquire the relative intensity of each region: alkyl C [0 to 50 parts per million (ppm)], O-alkyl C (50 to 110 ppm), aromatic C (110 to 165 ppm), and carboxylic C (165 to 220 ppm) (54).

To quantify SOM protection by minerals, Fe-bound SOC, which directly reflects the proportion of SOC associated with reactive Fe, was determined on the basis of the citrate-bicarbonate-dithionite (CBD) method (55). Briefly, in the reduction treatment, a solution containing trisodium citrate and sodium bicarbonate was added to 0.25 g of soil and heated to 80°C by water bath. A reducing agent, sodium dithionite, was then added, and the mixture was held at 80°C for 15 min. Instead of CBD extraction, soil samples in the control treatment were extracted with sodium chloride (NaCl) at an equivalent ionic strength. After rinsing the soil residues three times with 1 M NaCl, SOC content of the residues in each treatment was measured. Fe-bound SOC was then calculated as follows

$$\text{Fe-bound SOC (\%)} = \frac{\text{SOC}_{\text{NaCl}} - \text{SOC}_{\text{CBD}}}{\text{SOC}} \times 100 \quad (8)$$

where  $\text{SOC}_{\text{NaCl}}$  and  $\text{SOC}_{\text{CBD}}$  refer to the SOC content ( $\text{g kg}^{-1}$ ) of the control treatment and reduction treatment, respectively.

To determine SOM protection by aggregates, we isolated three SOM fractions to measure C distributions in each fraction. Specifically, using

the wet-sieving technique (56), 30 g of air-dried soil (<2 mm) was submerged in water for 5 min and then wet-sieved over 250 and 53  $\mu\text{m}$  of sieves, consecutively. The fraction collected on the 250- $\mu\text{m}$  sieve was macroaggregates (250 to 2000  $\mu\text{m}$ ), and that collected on the 53- $\mu\text{m}$  sieve was microaggregates (53 to 250  $\mu\text{m}$ ). The fraction in the remaining suspension was silt + clay (<53  $\mu\text{m}$ ). Each fraction was then dried at 60°C. After isolating sand in macroaggregates and microaggregates with sodium hexametaphosphate, SOC concentrations of the three fractions were measured. Of the three fractions, the proportions of SOC distributed in macroaggregates and microaggregates were used to quantify SOM protection by aggregates (27).

We adopted the PLFA approach to assess soil microbial abundance and community composition. PLFAs were extracted according to the protocol described by Bossio and Scow (57). With 19:0 (methyl nonadecanoate,  $\text{C}_{20}\text{H}_{40}\text{O}_2$ ) as the internal standard, samples were then analyzed with a gas chromatograph (Agilent 6850, Agilent Technologies, Santa Clara, CA, USA). The identification of the extracted fatty acid was based on a MIDI peak identification system (Microbial ID Inc., Newark, DE, USA). PLFAs specific to fungi (18:2 $\omega$ 6, 9c) and bacteria (i14:0, i15:0, a15:0, i16:0, a17:0, i17:0, 16:1 $\omega$ 7c, cy-17:0, 18:1 $\omega$ 7, cy19:0) were quantified (17). The composition of the microbial community was represented by the relative abundance of fungal PLFAs and F/B ratio.

### Statistical analyses

We conducted mixed effects models (R package: nlme) to examine the difference in  $Q_{10}$  values between the topsoil and the subsoil. In the model, site and soil depth were set as fixed factors, and depth nested in replicate was treated as a random factor. Having detected no interaction effect between site and soil depth (table S1), we used paired  $t$  tests to compare the means of physicochemical properties between the topsoil and the subsoil. Linear regression models were then performed to identify the relationships of  $Q_{10}$  with aggregate protection and microbial communities. Before the analyses, the variance inflation factor (VIF) was calculated to assess the collinearity of the variables (acceptable collinearity  $\text{VIF} \leq 2$ ) (58). On the basis of this criterion, the collinearity between SOC distribution in macroaggregates and microaggregates could be partly omitted ( $\text{VIF} = 1.6$ ), whereas the relative abundance of fungal PLFAs was closely correlated with F/B ( $\text{VIF} = 4.4$ ), and thus, only the former was included in the model.

To further analyze the relative importance of different variables, we conducted variation partitioning analysis (R package: vegan) to partition the effects of aggregate protection and microbial communities on  $Q_{10}$  in various C pools.  $\Delta Q_{10}$  ( $Q_{10 \text{ topsoil}} - Q_{10 \text{ subsoil}}$ ), the difference in  $Q_{10}$  between the topsoil and the subsoil) for the two manipulative experiments was then calculated to test the role of aggregate protection and microbial communities. A positive value of  $\Delta Q_{10}$  represents larger  $Q_{10}$  in the topsoil, while a negative value represents larger  $Q_{10}$  in the subsoil. The means of  $\Delta Q_{10}$  between control and crush/inoculation treatments were compared using paired  $t$  tests. The decrease in  $\Delta Q_{10}$  compared with the control indicates that crush/inoculation treatment reduces the difference in  $Q_{10}$  between the topsoil and the subsoil and vice versa. All of the statistical analyses were conducted with R version 3.2.1 (59), with a significance level of 0.05.

### SUPPLEMENTARY MATERIALS

Supplementary material for this article is available at <http://advances.sciencemag.org/cgi/content/full/5/7/eaau1218/DC1>

Fig. S1. Field soil sampling and laboratory incubation.

Fig. S2. Effects of microorganism reciprocal transplant on  $Q_{10}$  for the two soil depths.

Fig. S3. Changes in the cumulative respired soil C with incubation time.

Fig. S4. Comparison between modeled and measured soil C flux.

Table S1. Analysis of variance table for  $Q_{10}$  values from different sites and soil depths.

Table S2. Comparison of topsoil and subsoil microbial communities at three sites.

Table S3. Physicochemical characteristics in the two soil depths at three sites.

Table S4. Prior parameter ranges for C pool partitioning coefficients ( $f_i$ ), decay rates ( $k_i$ ), and temperature sensitivity ( $Q_{10}^i$ ).

## REFERENCES AND NOTES

- E. G. Jobbágy, R. B. Jackson, The vertical distribution of soil organic carbon and its relation to climate and vegetation. *Ecol. Appl.* **10**, 423–436 (2000).
- S. Fontaine, S. Barot, P. Barré, N. Bdioui, B. Mary, C. Rumpel, Stability of organic carbon in deep soil layers controlled by fresh carbon supply. *Nature* **450**, 277–280 (2007).
- E. A. Davidson, I. A. Janssens, Temperature sensitivity of soil carbon decomposition and feedbacks to climate change. *Nature* **440**, 165–173 (2006).
- T. W. Crowther, K. E. O. Todd-Brown, C. W. Rowe, W. R. Wieder, J. C. Carey, M. B. Machmuller, B. L. Snoek, S. Fang, G. Zhou, S. D. Allison, J. M. Blair, S. D. Bridgman, A. J. Burton, Y. Carrillo, P. B. Reich, J. S. Clark, A. T. Classen, F. A. Dijkstra, B. Elberling, B. A. Emmett, M. Estiarte, S. D. Frey, J. Guo, J. Harte, L. Jiang, B. R. Johnson, G. Kröel-Dulay, K. S. Larsen, H. Laudon, J. M. Lavallee, Y. Luo, M. Lupascu, L. N. Ma, S. Marhan, A. Michelsen, J. Mohan, S. Niu, E. Pendall, J. Peñuelas, L. Pfeifer-Meister, C. Poll, S. Reinsch, L. L. Reynolds, I. K. Schmidt, S. Sistla, N. W. Sokol, P. H. Templer, K. K. Treseder, J. M. Welker, M. A. Bradford, Quantifying global soil carbon losses in response to warming. *Nature* **540**, 104–108 (2016).
- C. E. Hicks Pries, C. Castanha, R. C. Porras, M. S. Torn, The whole-soil carbon flux in response to warming. *Science* **355**, 1420–1423 (2017).
- M. A. Bradford, W. R. Wieder, G. B. Bonan, N. Fierer, P. A. Raymond, T. W. Crowther, Managing uncertainty in soil carbon feedbacks to climate change. *Nat. Clim. Chang.* **6**, 751–758 (2016).
- T. Zhou, P. Shi, D. Hui, Y. Luo, Global pattern of temperature sensitivity of soil heterotrophic respiration ( $Q_{10}$ ) and its implications for carbon-climate feedback. *J. Geophys. Res.* **114**, G02016 (2009).
- E. Bosatta, G. I. Ågren, Soil organic matter quality interpreted thermodynamically. *Soil Biol. Biochem.* **31**, 1889–1891 (1999).
- C. Rumpel, I. Kögel-Knabner, Deep soil organic matter—A key but poorly understood component of terrestrial C cycle. *Plant Soil* **338**, 143–158 (2011).
- R. T. Conant, M. G. Ryan, G. I. Ågren, H. E. Birge, E. A. Davidson, P. E. Eliasson, S. E. Evans, S. D. Frey, C. P. Giardina, F. M. Hopkins, R. Hyvönen, M. U. F. Kirschbaum, J. M. Lavallee, J. Leifeld, W. J. Parton, J. Megan Steinweg, M. D. Wallenstein, J. Å. Martin Wetterstedt, M. A. Bradford, Temperature and soil organic matter decomposition rates - synthesis of current knowledge and a way forward. *Glob. Change Biol.* **17**, 3392–3404 (2011).
- J. A. J. Dungait, D. W. Hopkins, A. S. Gregory, A. P. Whitmore, Soil organic matter turnover is governed by accessibility not recalcitrance. *Glob. Change Biol.* **18**, 1781–1796 (2012).
- J. Lehmann, M. Kleber, The contentious nature of soil organic matter. *Nature* **528**, 60–68 (2015).
- M. W. I. Schmidt, M. S. Torn, S. Abiven, T. Dittmar, G. Guggenberger, I. A. Janssens, M. Kleber, I. Kögel-Knabner, J. Lehmann, D. A. C. Manning, P. Nannipieri, D. P. Rasse, S. Weiner, S. E. Trumbore, Persistence of soil organic matter as an ecosystem property. *Nature* **478**, 49–56 (2011).
- K. Karhu, M. D. Auffret, J. A. J. Dungait, D. W. Hopkins, J. I. Prosser, B. K. Singh, J.-A. Subke, P. A. Wookey, G. I. Ågren, M.-T. Sebastià, F. Gouriveau, G. Bergkvist, P. Meir, A. T. Nottingham, N. Salinas, I. P. Hartley, Temperature sensitivity of soil respiration rates enhanced by microbial community response. *Nature* **513**, 81–84 (2014).
- M. P. Waldrop, K. P. Wickland, R. White III, A. A. Berhe, J. W. Harden, V. E. Romanovsky, Molecular investigations into a globally important carbon pool: Permafrost-protected carbon in Alaskan soils. *Glob. Change Biol.* **16**, 2543–2554 (2010).
- J. Gillabel, B. Cebrian-Lopez, J. Six, R. Merckx, Experimental evidence for the attenuating effect of SOM protection on temperature sensitivity of SOM decomposition. *Glob. Change Biol.* **16**, 2789–2798 (2010).
- L. Chen, J. Liang, S. Qin, L. Liu, K. Fang, Y. Xu, J. Ding, F. Li, Y. Luo, Y. Yang, Determinants of carbon release from the active layer and permafrost deposits on the Tibetan Plateau. *Nat. Commun.* **7**, 13046 (2016).
- J. Balesdent, I. Basile-Doelsch, J. Chadoeuf, S. Cornu, D. Derrien, Z. Fekiacova, C. Hatté, Atmosphere-soil carbon transfer as a function of soil depth. *Nature* **559**, 599–602 (2018).
- J. Tian, J. Pausch, G. Yu, E. Blagodatskaya, Y. Gao, Y. Kuzyakov, Aggregate size and their disruption affect  $^{14}\text{C}$ -labeled glucose mineralization and priming effect. *Appl. Soil Ecol.* **90**, 1–10 (2015).
- C. C. Treat, W. M. Wollheim, R. K. Varner, A. S. Grandy, J. Talbot, S. Frohling, Temperature and peat type control  $\text{CO}_2$  and  $\text{CH}_4$  production in Alaskan permafrost peats. *Glob. Change Biol.* **20**, 2674–2686 (2014).
- W. Knorr, I. C. Prentice, J. I. House, E. A. Holland, Long-term sensitivity of soil carbon turnover to warming. *Nature* **433**, 298–301 (2005).
- R. T. Conant, R. A. Drijber, M. L. Haddix, W. J. Parton, E. A. Paul, A. F. Plante, J. Six, J. M. Steinweg, Sensitivity of organic matter decomposition to warming varies with its quality. *Glob. Change Biol.* **14**, 868–877 (2008).
- W. J. Parton, D. S. Schimel, C. V. Cole, D. S. Ojima, Analysis of factors controlling soil organic matter levels in Great Plains Grasslands. *Soil Sci. Soc. Am. J.* **51**, 1173–1179 (1987).
- D. S. Jenkinson, K. Coleman, The turnover of organic carbon in subsoils. Part 2. Modelling carbon turnover. *Eur. J. Soil Sci.* **59**, 400–413 (2008).
- X. Zhou, X. Xu, G. Zhou, Y. Luo, Temperature sensitivity of soil organic carbon decomposition increased with mean carbon residence time: Field incubation and data assimilation. *Glob. Change Biol.* **24**, 810–822 (2017).
- J. Liang, D. Li, Z. Shi, J. M. Tiedje, J. Zhou, E. A. G. Schuur, K. T. Konstantinidis, Y. Luo, Methods for estimating temperature sensitivity of soil organic matter based on incubation data: A comparative evaluation. *Soil Biol. Biochem.* **80**, 127–135 (2015).
- J. Six, R. T. Conant, E. A. Paul, K. Paustian, Stabilization mechanisms of soil organic matter: Implications for C-saturation of soils. *Plant Soil* **241**, 155–176 (2002).
- E. Blagodatskaya, X. Zheng, S. Blagodatsky, R. Wieg, M. Dannemann, K. Butterbach-Bahl, Oxygen and substrate availability interactively control the temperature sensitivity of  $\text{CO}_2$  and  $\text{N}_2\text{O}$  emission from soil. *Biol. Fertil. Soils* **50**, 775–783 (2014).
- E. Paterson, G. Osler, L. A. Dawson, T. Gebbing, A. Sim, B. Ord, Labile and recalcitrant plant fractions are utilised by distinct microbial communities in soil: Independent of the presence of roots and mycorrhizal fungi. *Soil Biol. Biochem.* **40**, 1103–1113 (2008).
- M. J. I. Briones, N. P. McNamara, J. Poskitt, S. E. Crow, N. J. Ostle, Interactive biotic and abiotic regulators of soil carbon cycling: Evidence from controlled climate experiments on peatland and boreal soils. *Glob. Change Biol.* **20**, 2971–2982 (2014).
- C. E. Hicks Pries, B. N. Sulman, C. West, C. O'Neill, E. Poppleton, R. C. Porras, C. Castanha, B. Zhu, D. B. Wiedemeier, M. S. Torn, Root litter decomposition slows with soil depth. *Soil Biol. Biochem.* **125**, 103–114 (2018).
- T. Shahzad, M. I. Rashid, V. Maire, S. Barot, N. Perveen, G. Alvarez, C. Mougou, S. Fontaine, Root penetration in deep soil layers stimulates mineralization of millennia-old organic carbon. *Soil Biol. Biochem.* **124**, 150–160 (2018).
- X. Pang, B. Zhu, X. Lü, W. Cheng, Labile substrate availability controls temperature sensitivity of organic carbon decomposition at different soil depths. *Biogeochemistry* **126**, 85–98 (2015).
- G. Alvarez, T. Shahzad, L. Andanson, M. Bahn, M. D. Wallenstein, S. Fontaine, Catalytic power of enzymes decreases with temperature: New insights for understanding soil C cycling and microbial ecology under warming. *Glob. Change Biol.* **24**, 4238–4250 (2018).
- P. Barré, A. F. Plante, L. Cécillon, S. Lutfalla, F. Baudin, S. Bernard, B. T. Christensen, T. Eglin, J. M. Fernandez, S. Houot, T. Kätterer, C. Le Guillou, A. Macdonald, F. van Oort, C. Chenu, The energetic and chemical signatures of persistent soil organic matter. *Biogeochemistry* **130**, 1–12 (2016).
- J. Lehmann, D. Solomon, J. Kinyangi, L. Dathe, S. Wirick, C. Jacobsen, Spatial complexity of soil organic matter forms at nanometre scales. *Nat. Geosci.* **1**, 238–242 (2008).
- N. P. McNamara, H. I. J. Black, N. A. Beresford, N. R. Parekh, Effects of acute gamma irradiation on chemical, physical and biological properties of soils. *Appl. Soil Ecol.* **24**, 117–132 (2003).
- B. Kéral, S. Fontaine, A. Lallemand, S. Revallot, H. Billard, G. Alvarez, F. Maestre, C. Amblard, A.-C. Lehours, Cellular and non-cellular mineralization of organic carbon in soils with contrasted physicochemical properties. *Soil Biol. Biochem.* **125**, 286–289 (2018).
- V. Maire, G. Alvarez, J. Colombet, A. Comby, R. Despinasse, E. Dubreucq, M. Joly, A.-C. Lehours, V. Perrier, T. Shahzad, S. Fontaine, An unknown oxidative metabolism substantially contributes to soil  $\text{CO}_2$  emissions. *Biogeochemistry* **10**, 1155–1167 (2013).
- W. R. Wieder, G. B. Bonan, S. D. Allison, Global soil carbon projections are improved by modelling microbial processes. *Nat. Clim. Chang.* **3**, 909–912 (2013).
- N. Perveen, S. Barot, G. Alvarez, K. Klumpp, R. Martin, A. Rapaport, D. Herfurth, F. Louault, S. Fontaine, Priming effect and microbial diversity in ecosystem functioning and response to global change: A modeling approach using the SYMPHONY model. *Glob. Change Biol.* **20**, 1174–1190 (2014).
- J. P. Schimel, M. N. Weintraub, The implications of exoenzyme activity on microbial carbon and nitrogen limitation in soil: A theoretical model. *Soil Biol. Biochem.* **35**, 549–563 (2003).
- W. R. Wieder, S. D. Allison, E. A. Davidson, K. Georgiou, O. Hararuk, Y. He, F. Hopkins, Y. Luo, M. J. Smith, B. Sulman, K. Todd-Brown, Y.-P. Wang, J. Xia, X. Xu, Explicitly representing soil microbial processes in Earth system models. *Global Biogeochem. Cycles* **29**, 1782–1800 (2015).



44. J. Ding, F. Li, G. Yang, L. Chen, B. Zhang, L. Liu, K. Fang, S. Qin, Y. Chen, Y. Peng, C. Ji, H. He, P. Smith, Y. Yang, The permafrost carbon inventory on the Tibetan Plateau: A new evaluation using deep sediment cores. *Glob. Change Biol.* **22**, 2688–2701 (2016).
45. H. Chen, Q. Zhu, C. Peng, N. Wu, Y. Wang, X. Fang, Y. Gao, D. Zhu, G. Yang, J. Tian, X. Kang, S. Piao, H. Ouyang, W. Xiang, Z. Luo, H. Jiang, X. Song, Y. Zhang, G. Yu, X. Zhao, P. Gong, T. Yao, J. Wu, The impacts of climate change and human activities on biogeochemical cycles on the Qinghai-Tibetan Plateau. *Glob. Change Biol.* **19**, 2940–2955 (2013).
46. J. Ding, L. Chen, B. Zhang, L. Liu, G. Yang, K. Fang, Y. Chen, F. Li, D. Kou, C. Ji, Y. Luo, Y. Yang, Linking temperature sensitivity of soil CO<sub>2</sub> release to substrate, environmental, and microbial properties across alpine ecosystems. *Global Biogeochem. Cycles* **30**, 1310–1323 (2016).
47. World Reference Base for Soil Resources, "International soil classification system for naming soils and creating legends for soil maps" (World Soil Resources Reports No. 106, Food and Agriculture Organization of the United Nations, 2015).
48. J. C. Neff, D. U. Hooper, Vegetation and climate controls on potential CO<sub>2</sub>, DOC and DON production in northern latitude soils. *Glob. Change Biol.* **8**, 872–884 (2002).
49. A. Rey, P. Jarvis, Modelling the effect of temperature on carbon mineralization rates across a network of European forest sites (FORCAST). *Glob. Change Biol.* **12**, 1894–1908 (2006).
50. C. Schädel, E. A. G. Schuur, R. Bracho, B. Elberling, C. Knoblauch, H. Lee, Y. Luo, G. R. Shaver, M. R. Turetsky, Circumpolar assessment of permafrost C quality and its vulnerability over time using long-term incubation data. *Glob. Change Biol.* **20**, 641–652 (2014).
51. W. K. Hastings, Monte Carlo sampling methods using Markov chains and their applications. *Biometrika* **57**, 97–109 (1970).
52. N. Metropolis, A. W. Rosenbluth, M. N. Rosenbluth, A. H. Teller, E. Teller, Equation of state calculations by fast computing machines. *J. Chem. Phys.* **21**, 1087–1092 (1953).
53. M. W. I. Schmidt, H. Knicker, P. G. Hatcher, I. Kögel-Knabner, Improvement of <sup>13</sup>C and <sup>15</sup>N CPMAS NMR spectra of bulk soils, particle size fractions and organic material by treatment with 10% hydrofluoric acid. *Eur. J. Soil Sci.* **48**, 319–328 (1997).
54. M. J. Simpson, A. J. Simpson, The chemical ecology of soil organic matter molecular constituents. *J. Chem. Ecol.* **38**, 768–784 (2012).
55. K. Lalonde, A. Mucci, A. Ouellet, Y. Gélinas, Preservation of organic matter in sediments promoted by iron. *Nature* **483**, 198–200 (2012).
56. J. Six, E. T. Elliott, K. Paustian, J. W. Doran, Aggregation and soil organic matter accumulation in cultivated and native grassland soils. *Soil Sci. Soc. Am. J.* **62**, 1367–1377 (1998).
57. D. A. Bossio, K. M. Scow, Impacts of carbon and flooding on soil microbial communities: Phospholipid fatty acid profiles and substrate utilization patterns. *Microb. Ecol.* **35**, 265–278 (1998).
58. T. A. Craney, J. G. Surlis, Model-dependent variance inflation factor cutoff values. *Qual. Eng.* **14**, 391–403 (2002).
59. R Development Core Team, *R: A Language and Environment for Statistical Computing* (R Foundation for Statistical Computing, 2015).

**Acknowledgments:** We thank members of the IBCAS Sampling Campaign Teams for their assistance in field investigation, and we appreciate two anonymous reviewers for their insightful comments on an early version of this manuscript. **Funding:** This work was supported by the Strategic Priority Research Program of the Chinese Academy of Sciences (XDA19070303); National Key R&D Program of China (2017YFC0503903); National Natural Science Foundation of China (31770557 and 31825006); Key Research Program of Frontier Sciences, Chinese Academy of Sciences (QYZDB-SSW-SMC049); and Chinese Academy of Sciences–Peking University Pioneer Cooperation Team. **Author contributions:** Y.Y. and L.C. conceived the idea. L.C., S.Q., and Y.Y. designed the research. S.Q., K.F., Q.Z., J.W., F.L., and J.Y. performed the experiments. S.Q. and L.C. analyzed the data. S.Q., Y.Y., and L.C. wrote the manuscript. **Competing interests:** The authors declare that they have no financial or other competing interests. **Data and materials availability:** All data needed to evaluate the conclusions in the paper are present in the paper and/or the Supplementary Materials. Additional data related to this paper may be requested from the corresponding author (yhyang@ibcas.ac.cn).

Submitted 8 May 2018

Accepted 6 June 2019

Published 10 July 2019

10.1126/sciadv.aau1218

**Citation:** S. Qin, L. Chen, K. Fang, Q. Zhang, J. Wang, F. Liu, J. Yu, Y. Yang, Temperature sensitivity of SOM decomposition governed by aggregate protection and microbial communities. *Sci. Adv.* **5**, eaau1218 (2019).

## Temperature sensitivity of SOM decomposition governed by aggregate protection and microbial communities

Shuqi Qin, Leiyi Chen, Kai Fang, Qiwen Zhang, Jun Wang, Futing Liu, Jianchun Yu and Yuanhe Yang

*Sci Adv* 5 (7), eaau1218.  
DOI: 10.1126/sciadv.aau1218

ARTICLE TOOLS	<a href="http://advances.sciencemag.org/content/5/7/eaau1218">http://advances.sciencemag.org/content/5/7/eaau1218</a>
SUPPLEMENTARY MATERIALS	<a href="http://advances.sciencemag.org/content/suppl/2019/07/08/5.7.eaau1218.DC1">http://advances.sciencemag.org/content/suppl/2019/07/08/5.7.eaau1218.DC1</a>
REFERENCES	This article cites 57 articles, 1 of which you can access for free <a href="http://advances.sciencemag.org/content/5/7/eaau1218#BIBL">http://advances.sciencemag.org/content/5/7/eaau1218#BIBL</a>
PERMISSIONS	<a href="http://www.sciencemag.org/help/reprints-and-permissions">http://www.sciencemag.org/help/reprints-and-permissions</a>

Use of this article is subject to the [Terms of Service](#)

---

*Science Advances* (ISSN 2375-2548) is published by the American Association for the Advancement of Science, 1200 New York Avenue NW, Washington, DC 20005. The title *Science Advances* is a registered trademark of AAAS.

Copyright © 2019 The Authors, some rights reserved; exclusive licensee American Association for the Advancement of Science. No claim to original U.S. Government Works. Distributed under a Creative Commons Attribution NonCommercial License 4.0 (CC BY-NC).